Indirect exchange interaction between magnetic impurities near the helical edge

V. D. Kurilovich,[1,2] P. D. Kurilovich,[1,2] and I. S. Burmistrov[1,3]
[1]*Moscow Institute of Physics and Technology, 141700 Moscow, Russia*
[2]*Skolkovo Institute of Science and Technology, 143026 Moscow, Russia*
[3]*L. D. Landau Institute for Theoretical Physics, Kosygina Street 2, 117940 Moscow, Russia*
(Received 26 December 2016; revised manuscript received 3 March 2017; published 27 March 2017)

The indirect exchange interaction between magnetic impurities located in the bulk of a two-dimensional topological insulator decays exponentially with the distance. The indirect exchange interaction for magnetic impurities mediated by the helical states at the edge of the topological insulator demonstrates behavior which is typical for the Ruderman-Kittel-Kasuya-Yosida interaction in a one-dimensional metal. We have shown that interference between the bulk and the edge states in the two-dimensional topological insulator results in existence of an unusual contribution to the indirect exchange interaction which, on the one hand, decays exponentially with a distance at the length scale controlled by the Fermi energy of the edge states and, on the other hand, oscillates with distance along the helical edge with the period determined by the Fermi wavelength. We found that this interference contribution to the indirect exchange interaction becomes dominant for such configurations of two magnetic impurities that one of them is situated close to the helical edge whereas the other one is located far away in the bulk.

DOI: 10.1103/PhysRevB.95.115430

I. INTRODUCTION

Two-dimensional (2D) topological insulators have attracted great attention recently due to existence of two spin-momentum locked edge states caused by a strong spin-orbit coupling [1,2]. Because of this peculiar structure of the edge states in a topological insulator (TI), a spin current can propagate along the edges. This current is the basis of the quantum spin Hall effect which was predicted theoretically [3,4] and observed experimentally [5] in HgTe/CdTe quantum wells. One of the remarkable features of the helical edge is the perfect transport along it which cannot be suppressed by any perturbation preserving the time-reversal symmetry (in the absence of interactions), e.g., by nonmagnetic impurities. In the presence of interactions backscattering is possible, which leads to suppression of the edge conductance at finite temperatures [6–8]. Moreover, the electron-electron interaction can lead to the edge reconstruction and spontaneous breakdown of the time-reversal protection of the perfect edge transport [9].

A local perturbation which breaks the time-reversal symmetry such as classical magnetic impurities can also provide a source for a spin-flipping scattering of the edge states and, consequently, can affect the transport properties [10,11]. Thus the transport along the helical edge is sensitive to the properties of a system of magnetic impurities distributed not far from the boundary of the 2D TI [12–15]. For rare magnetic impurities the main source of interaction between them is the indirect exchange interaction (IEI). If magnetic impurities are situated exactly at the edge of a 2D TI the IEI mediated by the helical states has been computed recently [16]. Its dependence on a distance resembles the Ruderman-Kittel-Kasuya-Yosida (RKKY) interaction for a one-dimensional metal [17–19]. We recall that the main features of the behavior of the RKKY interaction with the distance between the impurities are power-law decay and oscillations with period π/k_F where k_F denotes the Fermi wave vector of the helical states. The latter favors the formation of a spin-glass state at low temperatures. However, the spin structure of the IEI reflects a strong spin-orbit coupling which exists in a 2D TI: there is interaction between the in-plane components of the impurity spins only. We note that considerations of Ref. [16] ignore the fact that the edge states are composed from the electronlike states with the spin-$1/2$ and the holelike states with the spin-$3/2$ as well as the presence of bulk states.

In the opposite limit, when the magnetic impurities are located deep in the bulk of a 2D TI, typical semiconductor behavior of the IEI can be expected. The IEI in three-dimensional (3D) semiconductors with the chemical potential pinned to the gap was first studied by Bloembergen and Rowland [20]. At low temperatures the IEI between magnetic impurities was found to decay exponentially with the distance. In the simplest case of an isotropic spectrum with a minimum (maximum) of the conduction (valence) band at the Γ point the sign of the IEI is constant and ferromagnetic ordering of the magnetic impurities is favored (see Refs. [21,22] for a review).

Recently, the IEI between magnetic impurities situated far away from the edges of the 2D TI based on a CdTe/HgTe/CdTe quantum well (QW) has attracted a theoretical interest [23,24]. In this case the IEI has rather complicated spin structure and decays exponentially with the distance at low temperatures provided that the chemical potential is pinned to the gap. It involves anisotropic *XXZ* Heisenberg interaction, magnetic pseudodipole interaction, and Dzyaloshinsky-Moriya interaction [24]. Such spin structure is typical for systems with a strong spin-orbit coupling, e.g., for magnetic impurities at the surface of a 3D TI [25–32]. The presence of inversion asymmetry of the CdTe/HgTe/CdTe quantum well [33–36] results in even more complicated spin structure of the IEI, which becomes noninvariant under rotations in the plane of the QW. Additionally, oscillations of the IEI with the distance appear [24].

In this paper we study theoretically the indirect exchange interaction between magnetic impurities situated near the helical edge of a 2D topological insulator, based on the CdTe/HgTe/CdTe QW. We concentrate on the case of low temperatures and the chemical potential lying within the

energy gap of the bulk spectrum. Contrary to all previous studies we take into account simultaneously the edge and bulk states; the latter are modified by the presence of the edge. We find the following interesting features of the indirect exchange interaction in a 2D TI.

(i) The IEI between magnetic impurities can be split up into three parts: contribution of the Bloembergen-Rowland type due to the bulk states which decays exponentially with the distance; contribution due to the edge states which resembles RKKY interaction in a one-dimensional metal; and contribution due to an interference between bulk and edge states. Depending on positions of the magnetic impurities the IEI is dominated by one among three contributions.

(ii) The edge state contribution to the IEI involves in-plane spin components only, in agreement with Ref. [16].

(iii) The interference term in the IEI decays exponentially with the distance, but the decay length depends explicitly on the position of the chemical potential within the bulk gap.

The outline of the paper is as follows. In Sec. II we remind the reader of the Bernevig-Huges-Zhang Hamiltonian for 2D electron and hole states in the (001) symmetric CdTe/HgTe/CdTe QW and formulate the problem. In Sec. III we study the structure of bulk and edge states and compute the Matsubara Green's function. The results for the IEI are presented in Sec. IV. The discussion of the obtained results and conclusions are given in Sec. V. The technical details of derivation of different contributions to the IEI interaction are presented in the Appendices.

II. THE MODEL

We start from the Bernevig-Hughes-Zhang Hamiltonian which can be used to describe low-energy physics of electron and hole states in a 2D TI based on the (001) CdTe/HgTe/CdTe QW [4]. Written in the basis of spatially quantized states of the QW which are commonly denoted as $|E_1,+\rangle$, $|H_1,+\rangle$, $|E_1,-\rangle$, $|H_1,-\rangle$ (for details on structure of these states see Refs. [4,36,37]), it has the following form:

$$H_{\mathrm{BHZ}} = \varepsilon(k) + \begin{pmatrix} M(k) & Ak_+ & 0 & \Delta \\ Ak_- & -M(k) & -\Delta & 0 \\ 0 & -\Delta & M(k) & -Ak_- \\ \Delta & 0 & -Ak_+ & -M(k) \end{pmatrix}. \tag{1}$$

Here we introduce

$$\varepsilon(k) = C - D\left(k_x^2 + k_y^2\right), \quad M(k) = M - B\left(k_x^2 + k_y^2\right). \tag{2}$$

The parameters A, B, C, D, Δ, and M depend on the width d of the QW. The term Δ describes the interface and bulk inversion asymmetry and, generally, can be comparable to the gap M [36].

As it was shown in Ref. [24], the terms quadratic in the momentum in the Hamiltonian (1) are not important for the calculation of the IEI. Therefore we shall consider a simplified model given by the Hamiltonian (1) in which we set $B = D = 0$. The inversion asymmetry term Δ results in oscillating dependence of the IEI on the distance between magnetic impurities situated in the bulk of the QW [24]. In order to simplify the calculations of the IEI in the presence of the helical edge we neglect Δ in the present paper. Thus the Hamiltonian we shall work with is given by the following expression:

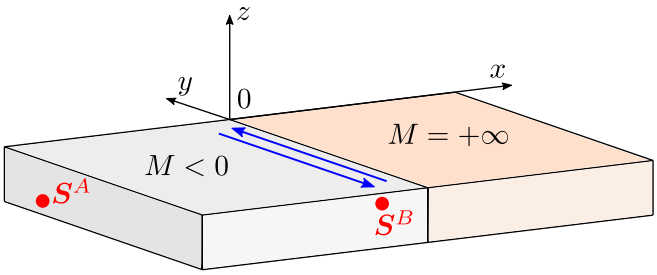

FIG. 1. Sketch of the setup. The 2D topological insulator (shaded gray) resides at $x < 0$. In this region the gap M is finite and negative. At $x > 0$ the gap is positive and infinite. A pair of helical states (blue lines) propagates along the edge. Magnetic impurities $\boldsymbol{S}^A$ and $\boldsymbol{S}^B$ are located inside the TI. Note that the positions of the impurities along the z axis determine corresponding electron-impurity coupling matrices.

$$H = \begin{pmatrix} M & Ak_+ & 0 & 0 \\ Ak_- & -M & 0 & 0 \\ 0 & 0 & M & -Ak_- \\ 0 & 0 & -Ak_+ & -M \end{pmatrix}. \tag{3}$$

The Hamiltonian of a magnetic impurity with the spin S situated at some point $\{x_0, y_0, z_0\}$ within the (001) QW reads [24]

$$\mathcal{V}_{\mathrm{imp}} = \mathcal{J}\delta(x - x_0)\delta(y - y_0), \tag{4}$$

where the matrix

$$\mathcal{J} = \begin{pmatrix} J_1 S_z & -iJ_0 S_+ & J_m S_- & 0 \\ iJ_0 S_- & J_2 S_z & 0 & 0 \\ J_m S_+ & 0 & -J_1 S_z & -iJ_0 S_- \\ 0 & 0 & iJ_0 S_+ & -J_2 S_z \end{pmatrix} \tag{5}$$

describes interaction with electron and hole states $|E_1,+\rangle$, $|H_1,+\rangle$, $|E_1,-\rangle$, $|H_1,-\rangle$. The coupling constants J_0, J_1, J_2, and J_m depend on z_0 and are determined by the envelope functions of spatially quantized states in the QW (see Ref. [24] for the details).

III. THE MATSUBARA GREEN'S FUNCTION

In order to evaluate the expression for the IEI it is convenient to use the Green's-function approach. Thus, we start from examining the Green's function for a 2D TI with a straight boundary situated at $x = 0$. We adopt the approach of Ref. [38] and assume that the gap M is a function of x such that $M(x)$ equals a negative constant for $x < 0$ and $M(x) = +\infty$ for $x > 0$ (see Fig. 1).

As we consider a system of noninteracting electrons described by the Hamiltonian (3) in the presence of the boundary at $x = 0$, it is necessary to take into account several important features. At first, there exist the edge states localized near the boundary which contribute to the Green's function. Secondly, the structure of the bulk states in the presence of the boundary differs from the case of an infinite sample in which

k_x is a good quantum number. It is convenient to evaluate the expression for the Green's function using Lehmann's representation:

$$\mathcal{G}(i\varepsilon_n,\boldsymbol{r},\boldsymbol{r}') = \sum_m \frac{\psi_m(\boldsymbol{r})\psi_m^\dagger(\boldsymbol{r}')}{i\varepsilon_n + \mu - \epsilon_m}, \tag{6}$$

where m enumerates eigenstates $\psi_m(\boldsymbol{r})$ of the Hamiltonian (3) with an energy ϵ_m. The chemical potential is denoted by μ and the Matsubara fermionic energy $\varepsilon_n = \pi T(2n+1)$.

Lehmann's representation suggests to split the Green's function into two parts: $\mathcal{G} = \mathcal{G}_{\text{edge}} + \mathcal{G}_{\text{bulk}}$. In $\mathcal{G}_{\text{edge}}$ ($\mathcal{G}_{\text{bulk}}$) summation over the edge (bulk) states is performed only.

A. The Green's function of the edge states

There exists a pair of the edge states connected via the time-reversal symmetry. For a given k_y one state is associated with the upper block of 4×4 Hamiltonian (3) and the other is associated with the lower one. They have the following form:

$$\psi_{\text{edge},\uparrow}(k_y,\boldsymbol{r}) = \begin{pmatrix}1\\ i\\ 0\\ 0\end{pmatrix}\frac{e^{ik_y y}}{\sqrt{2\pi\xi}}e^{-|x|/\xi}\theta(-x), \tag{7}$$

$$\psi_{\text{edge},\downarrow}(k_y,\boldsymbol{r}) = \begin{pmatrix}0\\ 0\\ 1\\ -i\end{pmatrix}\frac{e^{ik_y y}}{\sqrt{2\pi\xi}}e^{-|x|/\xi}\theta(-x), \tag{8}$$

where $\xi = A/|M|$ and $\theta(x)$ denotes the Heaviside step function. The absolute values of x in the exponents in Eqs. (7) and (8) indicate that the topological insulator is situated in the region with $x<0$.

The energy spectrum of the edge states is linear in the momentum: $\epsilon_{\text{edge},\uparrow/\downarrow}(k_y) = \pm Ak_y$. Integrating over the momentum k_y, we find

$$\mathcal{G}_{\text{edge}} = G^{\uparrow}_{\text{edge}} + G^{\downarrow}_{\text{edge}}, \tag{9}$$

where

$$\begin{aligned} &G^{\uparrow/\downarrow}_{\text{edge}}(i\varepsilon,\boldsymbol{r},\boldsymbol{r}') \\ &= \pm\frac{i|M|}{A^2}e^{-|x+x'|/\xi\pm(\varepsilon-i\mu)(y-y')/A}\theta(-x)\theta(-x') \\ &\quad\times[\theta(y-y')\theta(\mp\varepsilon)-\theta(y'-y)\theta(\pm\varepsilon)]\Gamma_\pm. \end{aligned} \tag{10}$$

Here the matrices $\Gamma_\pm$ are defined as follows:

$$\Gamma_+ = \begin{pmatrix}1 & -i & 0 & 0\\ i & 1 & 0 & 0\\ 0 & 0 & 0 & 0\\ 0 & 0 & 0 & 0\end{pmatrix},$$

$$\Gamma_- = \begin{pmatrix}0 & 0 & 0 & 0\\ 0 & 0 & 0 & 0\\ 0 & 0 & 1 & i\\ 0 & 0 & -i & 1\end{pmatrix}. \tag{11}$$

B. The Green's function of the bulk states

Now we discuss the structure of the bulk states in the presence of the boundary as well as the bulk part of the Green's function. There are four bulk states for the Hamiltonian (3). Two of them have positive energy, $\epsilon^{+}_{\text{bulk},\uparrow/\downarrow}(k) = \mathcal{E}(k)$ where $\mathcal{E}(k) = \sqrt{M^2 + A^2k^2}$, and two have negative energy, $\epsilon^{-}_{\text{bulk},\uparrow/\downarrow}(k) = -\mathcal{E}(k)$. It is convenient to introduce the following functions:

$$f_x^{\pm}(\boldsymbol{k}) = \frac{(Ak_\pm \pm i(\mathcal{E}(k)\mp|M|))e^{ik_x x} + \text{c.c.}}{2\sqrt{\mathcal{E}(k)(\mathcal{E}(k)+Ak_y)}}\theta(-x), \tag{12}$$

where $k_\pm = k_x \pm ik_y$. In terms of these functions one can present the bulk eigenstates as

$$\psi^{\pm}_{\text{bulk},\uparrow}(\boldsymbol{k},\boldsymbol{r}) = \begin{pmatrix}\pm f_x^{\pm}(\pm\boldsymbol{k})\\ \pm i f_x^{\mp}(\pm\boldsymbol{k})\\ 0\\ 0\end{pmatrix}\frac{e^{ik_y y}}{2\pi},$$

$$\psi^{\pm}_{\text{bulk},\downarrow}(\boldsymbol{k},\boldsymbol{r}) = \begin{pmatrix}0\\ 0\\ \mp f_x^{\pm}(\mp\boldsymbol{k})\\ \pm i f_x^{\mp}(\mp\boldsymbol{k})\end{pmatrix}\frac{e^{ik_y y}}{2\pi}. \tag{13}$$

The upper index "$\pm$" indicates whether the electron (+) or hole (−) band is concerned. The Green's function of the bulk states can be written in the following form:

$$\mathcal{G}_{\text{bulk}}(i\varepsilon,\boldsymbol{r},\boldsymbol{r}') = \sum_{s=\pm}\int\frac{d^2\boldsymbol{k}}{(2\pi)^2}e^{ik_y(y-y')}\frac{\theta(k_x)\mathcal{B}_s(\boldsymbol{k},x,x')}{i\varepsilon+\mu-s\mathcal{E}(k)}, \tag{14}$$

where $\mathcal{B}_s$ is the following 4×4 block-diagonal matrix:

$$\mathcal{B}_s(\boldsymbol{k},x,x') = \begin{pmatrix}\hat{b}_s(s\boldsymbol{k},x,x') & \hat{0}\\ \hat{0} & \hat{b}_s^T(-s\boldsymbol{k},x',x)\end{pmatrix},$$

$$\hat{b}_s(\boldsymbol{k},x,x') = \begin{pmatrix}f_x^s(\boldsymbol{k})f_{x'}^s(\boldsymbol{k}) & -if_x^s(\boldsymbol{k})f_{x'}^{-s}(\boldsymbol{k})\\ if_x^{-s}(\boldsymbol{k})f_{x'}^s(\boldsymbol{k}) & f_x^{-s}(\boldsymbol{k})f_{x'}^{-s}(\boldsymbol{k})\end{pmatrix}. \tag{15}$$

The superscript T denotes the matrix transposition.

IV. THE INDIRECT EXCHANGE INTERACTION

Let us now turn to the calculation of the indirect exchange interaction in case of the chemical potential lying in the bulk spectrum gap, $|\mu|<|M|$. To the second order in $\mathcal{J}$ the IEI is given by a polarization operator diagram. The corresponding effective Hamiltonian that describes the interaction of two magnetic impurities situated at points $\{\boldsymbol{R}_A,z_A\}$ and $\{\boldsymbol{R}_B,z_B\}$ (see Fig. 1) can be written as

$$H_{\text{IEI}} = T\sum_{\varepsilon_n}\text{Tr}\,\mathcal{J}^A\mathcal{G}(i\varepsilon_n,\boldsymbol{R}_A,\boldsymbol{R}_B)\mathcal{J}^B\mathcal{G}(i\varepsilon_n,\boldsymbol{R}_B,\boldsymbol{R}_A). \tag{16}$$

Here $\mathcal{J}^A$ ($\mathcal{J}^B$) is the electron-impurity interaction matrix (5) which depends on the position z_A (z_B) of the impurity in the z direction. In this paper we focus on the case of the zero temperature only. Thus, we shall replace the summation over the Matsubara frequencies in Eq. (16) by the integration.

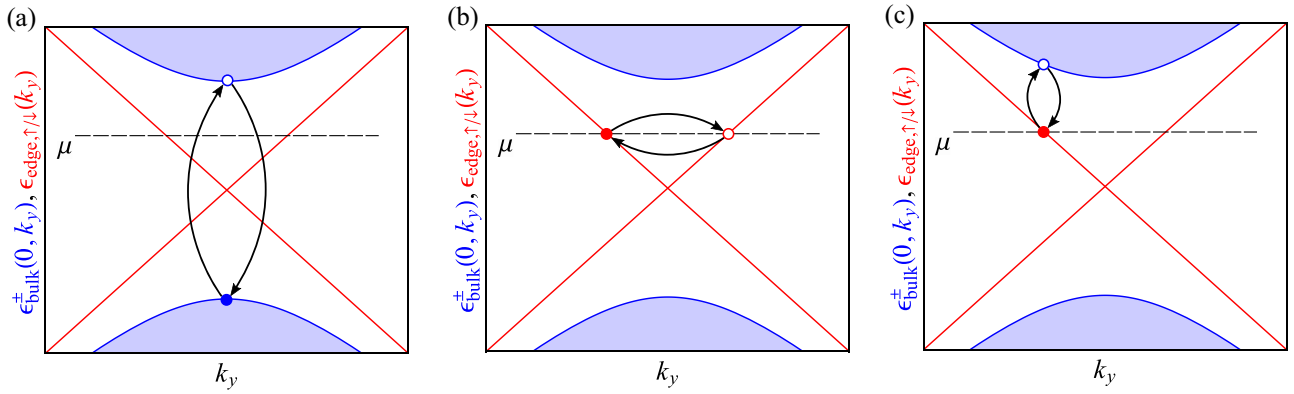

FIG. 2. A sketch of electron transitions that determine different types of the IEI: (a) bulk states mediated exchange, (b) edge states mediated exchange, and (c) interference contribution to the IEI. The bulk bands (depicted in blue) are located between the branches of edge states (red lines). The chemical potential is depicted with a horizontal dashed line. See text.

Since the Hamiltonian (16) involves a product of two Green's functions under the sign of Tr and each of them is a sum of the edge and bulk contributions, one can decompose the IEI as a sum of the following three terms:

$$H_{\rm IEI} = H_{\rm IEI}^{\rm bulk} + H_{\rm IEI}^{\rm edge} + H_{\rm IEI}^{\rm int}. \tag{17}$$

The first term in the right-hand side of this equation, $H_{\rm IEI}^{\rm bulk}$, is related to the bulk states only: it involves the product of two bulk Green's functions $\mathcal{G}_{\rm bulk}$. The second term, $H_{\rm IEI}^{\rm edge}$, is related to the edge states. It contains the edge Green's function, $\mathcal{G}_{\rm edge}$, only. The last term, $H_{\rm IEI}^{\rm int}$, describes the interference between the bulk and the edge states and involves the edge and bulk Green's functions simultaneously.

Each of these contributions has clear physical interpretation. The contribution to the IEI due to the bulk states, $H_{\rm IEI}^{\rm bulk}$, is associated with the virtual transitions of quasiparticles from the valence to the conduction band [a schematic illustration is presented in Fig. 2(a)]. These virtual processes are limited in time: the excited quasiparticle can reside in the conduction band over time inversely proportional to the band gap $\sim 1/|M|$, as dictated by the uncertainty principle. During this time, the quasiparticle can move for a spatial distance of the order of $A/|M|$. Therefore, the contribution $H_{\rm IEI}^{\rm bulk}$ is short ranged with the characteristic distance $\xi \sim A/|M|$.

The contribution to the IEI due to the edge states, $H_{\rm IEI}^{\rm edge}$, is associated with the transitions between different chiral branches of the edge spectrum [see Fig. 2(b)]. There is no energy gap to suppress these processes. Hence, the typical 1D metal behavior is expected for $H_{\rm IEI}^{\rm edge}$.

The interference contribution to the IEI, $H_{\rm IEI}$, is caused by the virtual transitions of quasiparticles between the edge states located below the chemical potential to the conduction band (as well as the transitions from the valence band to the edge states above chemical potential). These virtual processes are constrained in time by the uncertainty principle, and, therefore, a finite-ranged IEI is expected. However, in contrast to $H_{\rm IEI}^{\rm bulk}$, the energy gap that controls these transitions depends explicitly on the position of the chemical potential within the bulk gap [see Fig. 2(c)]. Hence, the range of $H_{\rm IEI}$ is expected to depend on the position of the chemical potential with respect to the bottom of the conduction band or the top of the valence band.

Before proceeding with the results for the three different contributions to the IEI, let us briefly discuss the notations. Hereinafter, we denote $\boldsymbol{R}_{A/B} \equiv (x_{A/B}, y_{A/B})$, $\boldsymbol{R} = \boldsymbol{R}_A - \boldsymbol{R}_B \equiv (x_{AB}, y_{AB})$, $\boldsymbol{n} = \boldsymbol{R}/R$, $\overline{x}_{AB} \equiv x_A + x_B$, $\overline{\boldsymbol{R}} = (\overline{x}_{AB}, y_{AB})$, and $\boldsymbol{v} = \overline{\boldsymbol{R}}/\overline{R}$, where $\overline{R} = \sqrt{y_{AB}^2 + \overline{x}_{AB}^2}$. In addition, we assume below that $y_{AB} > 0$.

A. Bulk and edge contributions to the IEI

The part of the IEI mediated by the bulk states has the complex form with nontrivial spin structure in general. In the absence of the boundary, the asymptotic expression for the IEI at the distances $R \gg \xi$ reads [24]

$$\begin{aligned} H_{\rm IEI}^{\rm bulk} = \frac{1}{|M|\xi^4}\left(\frac{\xi}{4\pi R}\right)^{3/2} e^{-2R/\xi}\big\{ & J_m^A J_m^A (\boldsymbol{S}_\parallel^A \cdot \boldsymbol{S}_\parallel^B) \\ & + 2\big[J_0^A J_z^B (\boldsymbol{S}_\parallel^A \cdot \boldsymbol{n}) S_z^B - J_z^A J_0^B S_z^A (\boldsymbol{S}_\parallel^B \cdot \boldsymbol{n})\big] \\ & - 4 J_0^A J_0^B \big(\boldsymbol{S}_\parallel^A \cdot \boldsymbol{n}\big)\big(\boldsymbol{S}_\parallel^B \cdot \boldsymbol{n}\big) + J_z^A J_z^B S_z^A S_z^B \big\}, \end{aligned} \tag{18}$$

where $J_z^{A/B} = J_1^{A/B} + J_2^{A/B}$. In the presence of the boundary the bulk states acquire nontrivial structure, Eqs. (13), that complicates the form of the IEI. The large distance asymptote of the full expression is presented in Appendix A. Additional terms, which appear, can be interpreted as the interaction between a magnetic impurity and the mirror image of the other impurity with respect to the boundary. (This is somewhat similar to the appearance of the mirror charges in electrostatics problems with the boundary.) These additional terms in the IEI decay in a different way: $\sim \exp[-(R+\overline{R})/\xi]$ and $\sim \exp(-2\overline{R}/\xi)$. Therefore, in the presence of the boundary Eq. (18) is valid provided the following inequalities are satisfied:

$$|x_A|, |x_B| \gg \xi. \tag{19}$$

The result (18) has been derived for the zero temperature. At finite temperature, this result is valid provided the following inequality holds [24]:

$$\frac{M^2}{T^2} \min\left\{1, \frac{T}{|\mu|}\left(1 - \frac{\mu^2}{M^2}\right)\right\} \gg \frac{R}{\xi} \gg 1. \tag{20}$$

If the condition above is satisfied, the intraband transitions, that become possible at finite temperature only, are negligible,

and the IEI mediated by the bulk states is still dominated by the interband transitions.

The expression for the contribution to the IEI due to the edge states only can be derived exactly at $T = 0$ within the help of Eqs. (9) and (10). The result is as follows:

$$H_{\rm edge}^{\rm IEI} = -\frac{e^{-2|\bar{x}_{AB}|/\xi}}{2\pi y_{AB}|M|\xi^3} J_m^A J_m^B [\cos(2k_F y_{AB})(\mathbf{S}_{||}^A \cdot \mathbf{S}_{||}^B) + \sin(2k_F y_{AB})[\mathbf{S}^A \times \mathbf{S}^B]_z], \quad (21)$$

where $k_F = \mu/A$ denotes the Fermi wave vector of the edge states. We mention that our result (21) for magnetic impurities situated exactly at the boundary, $x_A = x_B = 0$ coincides with the result derived in Ref. [16]. We note that a magnetic impurity situated away from the boundary interacts by means of the helical edge states with the mirror image of the other impurity with respect to the boundary only. This is the consequence of the absence of the translational invariance perpendicular to the boundary (along the x axis). The dependence of the IEI mediated by the edge states has a typical one-dimensional metallic behavior: it decays inversely proportionally to the distance and oscillates in space with the period π/k_F. A feature of the result (21) is that the edge contribution to the IEI couples in-plane components of the impurity spins only. This peculiarity could be expected from the explicit form of the electron-impurity interaction matrix (5). Indeed, this part of the IEI is mediated by the processes in which the chirality of the edge states changes. Such transition between chiral branches is associated with a spin flip. The only terms in Eq. (5) that allow for the spin flips are the terms $J_m S_+$ and $J_m S_-$ which contain only in-plane components of the impurity spin. Hence, only in-plane components of the impurity spin are present in the IEI mediated by the edge states. We will discuss later why this behavior may be crucial for the IEI if the on-site spin anisotropy is present.

At finite temperature one can perform summation over Matsubara frequencies in Eq. (16). Then one finds that at distances $|y_{AB}|/\xi \gg |M|/(\pi T)$ the contribution to the IEI due to the edge states decays exponentially as $\exp[-2\pi T|y_{AB}|/(\xi|M|)]$. This additional suppression of $H_{\rm IEI}^{\rm edge}$ is not important provided the following inequality holds:

$$|y_{AB}|/\xi \ll |M|/(\pi T). \quad (22)$$

Therefore, at finite temperature the result (21) is valid at distances $|y_{AB}|$ restricted from above by condition (22).

B. Interference contribution to the IEI

The evaluation of the interference contribution to the IEI is complicated for an arbitrary disposition of the magnetic impurities. In order to obtain analytic results we consider two limiting cases: (i) at least one of the impurities is situated far away from the boundary and (ii) both impurities are located near the boundary. In addition, we assume that the chemical potential is not pinned to the center of the bulk gap, $\mu \neq 0$. For $\mu = 0$ the interference contribution has the same decay length as the bulk contribution and, thus, is of no special interest.

1. A magnetic impurity away from the boundary

We start from the case when at least one of the impurities is located far away from the boundary, $|x_A| \gg \xi$ or $|x_B| \gg \xi$. In order to obtain the expression for the interference contribution to the IEI in this case, it is convenient to separate the bulk Green's function into two parts:

$$\mathcal{G}_{\rm bulk} = \mathcal{G}_{\rm bulk}^{\rm i} + \mathcal{G}_{\rm bulk}^{\rm ni}, \quad (23)$$

where $\mathcal{G}_{\rm bulk}^{\rm i}$ ($\mathcal{G}_{\rm bulk}^{\rm ni}$) is the translationally invariant (noninvariant) part. The translationally invariant part of the bulk Green's function depends only on the relative position of the impurities, while the translationally noninvariant part is suppressed when both impurities are far away from the edge.

Splitting the bulk Green's function into translationally invariant and noninvariant parts allows us to express the interference contribution to the IEI as a sum of the two terms:

$$H_{\rm IEI}^{\rm int} = H_{\rm IEI}^{\rm int,\,i} + H_{\rm IEI}^{\rm int,\,ni}, \quad (24)$$

where the former is given by the product of the edge Green's function and the invariant part of the bulk Green's function, while the latter can be expressed as the product of the edge Green's function and the noninvariant part of the bulk Green's function.

For the sake of convenience, we introduce a set of coupling constants K defined as follows:

$$H_{\rm IEI}^{\rm int,\,i/ni} = \sum_{a,b=x,y,z} S_a^A K_{ab}^{\rm int,\,i/ni} S_b^B. \quad (25)$$

The large distance asymptote of the matrix $K^{\rm int,\,i}$ which determines the invariant part of the interference contribution to the IEI is given by the following expressions (see Appendix B):

$$\begin{aligned}
K_{xx}^{\rm int,i} &= 2F_\mu(\boldsymbol{R})g_\mu(y_{AB})\big[(1-\sin\theta_\mu)J_m^A J_m^B - 2(\sin\theta_\mu - i\cos\theta_\mu n_y)J_0^A J_0^B\big] + \text{c.c.},\\
K_{yy}^{\rm int,i} &= 2F_\mu(\boldsymbol{R})g_\mu(y_{AB})\big[(1-\sin\theta_\mu)J_m^A J_m^B - 2(\sin\theta_\mu + i\cos\theta_\mu n_y)J_0^A J_0^B\big] + \text{c.c.},\\
K_{zz}^{\rm int,i} &= 2F_\mu(\boldsymbol{R})g_\mu(y_{AB})\big[(1-\sin\theta_\mu)J_1^A J_1^B - (1+\sin\theta_\mu)J_2^A J_2^B + \cos\theta_\mu n_+ J_1^A J_2^B - \cos\theta_\mu n_- J_2^A J_1^B)\big] + \text{c.c.},\\
K_{xy}^{\rm int,i} &= 2iF_\mu(\boldsymbol{R})g_\mu(y_{AB})\big[(1-\sin\theta_\mu)J_m^A J_m^B + 2J_0^A J_0^B(1-\cos\theta_\mu n_x)\big] + \text{c.c.},\\
K_{xz}^{\rm int,i} &= 2F_\mu(\boldsymbol{R})g_\mu(y_{AB})\big[(1-\sin\theta_\mu - \cos\theta_\mu n_-)J_0^A J_1^B - (1+\sin\theta_\mu - \cos\theta_\mu n_+)J_0^A J_2^B\big] + \text{c.c.},\\
K_{yz}^{\rm int,i} &= -2iF_\mu(\boldsymbol{R})g_\mu(y_{AB})\big[(1-\sin\theta_\mu + \cos\theta_\mu n_-)J_0^A J_1^B + (1+\sin\theta_\mu + \cos\theta_\mu n_+)J_0^A J_2^B\big] + \text{c.c.}
\end{aligned} \quad (26)$$

Here $n_\pm = n_x \pm i n_y$ and the phase θ_μ satisfies the following relations:

$$\sin\theta_\mu = \frac{\mu}{|M|}, \quad \cos\theta_\mu = \sqrt{1-\frac{\mu^2}{M^2}}. \tag{27}$$

The dimensionless function $g_\mu(y)$ is defined as follows:

$$g_\mu(y) = \frac{e^{ik_F y}}{\sin\theta_\mu + i\cos\theta_\mu n_y}. \tag{28}$$

The function

$$F_\mu(\boldsymbol{R}) = \frac{\sqrt{\cos\theta_\mu}}{2|M|\xi^4}\left(\frac{\xi}{2\pi R}\right)^{3/2} e^{-|\overline{x}_{AB}|/\xi - R/\xi_\mu} \tag{29}$$

determines the spatial decay of the translationally invariant part of the interference contribution to the IEI. The corresponding decay length scale is given by

$$\xi_\mu = \xi/\sqrt{1-\mu^2/M^2}. \tag{30}$$

The remaining set of matrix elements of $K_{ab}^{\text{int, i}}$ can be obtained from the ones presented above: $K_{yx}^{\text{int, i}}$, $K_{yz}^{\text{int, i}}$, and $K_{zx}^{\text{int, i}}$ can be read from $K_{xy}^{\text{int, i}}$, $K_{zy}^{\text{int, i}}$, and $K_{xz}^{\text{int, i}}$, respectively, upon change of $\boldsymbol{R}$ to $-\boldsymbol{R}$ and swap of subscripts A and B.

Appearance of the decay length ξ_μ that depends explicitly on the position of the chemical potential μ is in agreement with qualitative arguments [see Fig. 2(c)]. This feature allows one to tune electrically the range of the interference interaction. It is worth mentioning that ξ_μ diverges as the chemical potential approaches the bulk spectrum.

In addition to the term $-R/\xi_\mu$ in the exponent of $F_\mu(\boldsymbol{R})$ there is a term $-|\overline{x}_{AB}|/\xi$, which induces the decay of the interference contribution to the IEI for the impurities situated far away from the edge. Besides the features mentioned above, the matrix elements $K_{ab}^{\text{int,i}}$ oscillate with the distance along the edge with a period $2\pi/k_F$ which is two times longer than the period of oscillations of the contribution to the IEI mediated by the edge states only. These particular features of the interference contribution to the IEI are descendants of the properties of the edge Green's function.

The result (26) is obtained in the saddle-point approximation and is valid for the large distances

$$R \gg \xi_\mu/\sin^2\theta_\mu = \frac{\xi}{\frac{\mu^2}{M^2}\sqrt{1-\frac{\mu^2}{M^2}}}. \tag{31}$$

Note that the right-hand side of this inequality diverges at $\mu = \pm|M|$, i.e., when the chemical potential touches the bulk bands, as well as at $\mu = 0$. The latter implies that the result (26) is not applicable when the chemical potential is pinned exactly to the middle of the bulk gap. This limitation of our results has no physical meaning and is due to the saddle-point treatment of the integrals in the course of calculations (see Appendix B for details). However, the case of the chemical potential close to the middle of the bulk gap is not interesting since in this case $\xi_\mu \approx \xi$ and, consequently, the interference contribution to the IEI is smaller than the contribution due to either the edge states or the bulk states (see discussion in Sec. V below).

At finite temperatures the result (26) is valid for not too large distance between the impurities:

$$\left(x_{AB}^2\sin^2\theta_\mu + y_{AB}^2\right)^{1/2}/\xi \ll |M|/(\pi T). \tag{32}$$

The matrix elements of $K_{ab}^{\text{int, ni}}$ of the noninvariant part of the interference contribution to the IEI are given by the following expressions (see Appendix B):

$$\begin{aligned}
K_{xx}^{\text{int, ni}} &= -2F_\mu(\overline{\boldsymbol{R}})\overline{g_\mu}(y_{AB})\left[(u_\mu - u_{-\mu}^* + iv_\mu + iv_{-\mu}^*)J_0^A J_0^B + u_\mu^* J_m^A J_m^B\right] + \text{c.c.},\\
K_{yy}^{\text{int, ni}} &= -2F_\mu(\overline{\boldsymbol{R}})\overline{g_\mu}(y_{AB})\left[(u_\mu - u_{-\mu}^* - iv_\mu - iv_{-\mu}^*)J_0^A J_0^B + u_\mu^* J_m^A J_m^B\right] + \text{c.c.},\\
K_{zz}^{\text{int, ni}} &= -2F_\mu(\overline{\boldsymbol{R}})\overline{g_\mu}(y_{AB})\left[u_\mu J_1^A J_1^B - u_{-\mu}^* J_2^A J_2^B + iv_\mu J_1^A J_2^B + iv_{-\mu}^* J_2^A J_1^B\right] + \text{c.c.},\\
K_{xy}^{\text{int, ni}} &= -2iF_\mu(\overline{\boldsymbol{R}})\overline{g_\mu}(y_{AB})\left[(u_\mu + u_{-\mu}^* - iv_\mu + iv_{-\mu}^*)J_0^A J_0^B + u_\mu^* J_m^A J_m^B\right] + \text{c.c.},\\
K_{xz}^{\text{int, ni}} &= -2F_\mu(\overline{\boldsymbol{R}})\overline{g_\mu}(y_{AB})\left[(u_\mu + iv_{-\mu}^*)J_0^A J_1^B - (u_{-\mu}^* - iv_\mu)J_0^A J_2^B\right] + \text{c.c.},\\
K_{yz}^{\text{int, ni}} &= 2iF_\mu(\overline{\boldsymbol{R}})\overline{g_\mu}(y_{AB})\left[(u_\mu - iv_{-\mu}^*)J_0^A J_1^B + (u_{-\mu}^* + iv_\mu)J_0^A J_2^B\right] + \text{c.c.}
\end{aligned} \tag{33}$$

Here $v_\pm = v_x \pm i v_y$ and we introduce the dimensionless functions

$$\overline{g_\mu}(y) = \frac{e^{ik_F y}}{\sin\theta_\mu + i\cos\theta_\mu v_y} \tag{34}$$

and

$$\begin{aligned}
u_\mu &= -\frac{1}{2}\frac{(v_+\cos\theta_\mu + \sin\theta_\mu - 1)^2}{\sin\theta_\mu + iv_y\cos\theta_\mu},\\
v_\mu &= \frac{i\cos\theta_\mu(\cos\theta_\mu - v_x - iv_y\sin\theta_\mu)}{\sin\theta_\mu + iv_y\cos\theta_\mu}.
\end{aligned} \tag{35}$$

The elements $K_{yx}^{\text{int, ni}}$ and $K_{yz}^{\text{int, ni}}$ are equal to $-K_{xy}^{\text{int, ni}}$ and $-K_{zy}^{\text{int, ni}}$ after interchange of subscripts A and B as well as v_μ and $v_{-\mu}^*$, respectively. The element $K_{zx}^{\text{int, ni}}$ can be obtained from $K_{xz}^{\text{int, ni}}$ by swapping A to B and v_μ to $v_{-\mu}^*$.

The applicability conditions for the answer for the noninvariant part of the interference contribution to the IEI are similar to Eqs. (31) and (32): $\overline{R} \gg \xi_\mu/\sin^2\theta_\mu$ and $(\overline{x}_{AB}^2\sin^2\theta_\mu + y_{AB}^2)^{1/2}/\xi \ll |M|/(\pi T)$. Typically, the noninvariant part of the interference contribution to the IEI is smaller than the invariant part. However, if one of the impurities is situated strictly at the edge, such that $R = \overline{R}$ and $|x_{AB}| = |\overline{x}_{AB}|$, the spatial decay of the noninvariant part is exactly the same

as the spatial decay of the invariant part. Next, as one can check, in the case of both impurities located exactly at the boundary, $x_A = x_B = 0$, the invariant and noninvariant parts of the interference contribution to the IEI compensate each other. Therefore, for the case of both impurities situated exactly at the edge one needs to compute the asymptotic expressions for $K_{ab}^{\rm int}$ more accurately.

2. *Magnetic impurities situated at the edge*

Within the second-order expansion in the steepest descent method we calculate the interference contribution to the IEI for two impurities which are located strictly at the edge, $x_A = x_B = 0$ (see Appendix C). The corresponding Hamiltonian reads

$$H_{\rm IEI}^{\rm int} = -\frac{4\xi\cos\theta_\mu}{y_{AB}} F_\mu(0,y_{AB})\Big\{J_m^A J_m^B\Big[\cos(k_F y_{AB})(\boldsymbol{S}_{||}^A\cdot\boldsymbol{S}_{||}^B) - \sin(k_F y_{AB})[\boldsymbol{S}^A\times\boldsymbol{S}^B]_z\Big] - \Big[4J_0^A J_0^B S_x^A S_x^B + 2\big(J_0^A J_z^B S_x^A S_z^B + J_0^B J_z^A S_x^B S_z^A\big) + J_z^A J_z^B S_z^A S_z^B\Big]\cos(k_F y_{AB}+2\theta_\mu)\Big\}. \quad (36)$$

We mention that the power-law dependence of the result (36) on the distance is $y_{AB}^{-5/2}$ rather than $y_{AB}^{-3/2}$. The additional power is due to the next order expansion in the steepest descent method. At finite temperature the condition of applicability of the result (36) is similar to that for the contribution due to the edge states, $|y_{AB}|/\xi \ll |M|/(\pi T)$.

For impurities situated close to the edge, $|x_A|, |x_B| \ll \xi$, the interference contribution to the IEI is given as a sum of the results (26) and (33) as well as the generalization of the result (36). It has features similar to the result (36): the exponential decay at the length scale ξ_μ as well as oscillations with the spatial period $2\pi/k_F$.

V. DISCUSSION AND CONCLUSIONS

The results for the IEI reported above were derived within the lowest order in the exchange coupling constants J_0, J_1, J_2, and J_m. The typical value of the IEI is given by the energy scale $T_* \sim \max\{J_z^2, J_0^2, J_m^2\}/(|M|\xi^4)$ which can be estimated to be of the order of 10^{-3}–10^{-4} K for the manganese impurities in the CdTe/HgTe/CdTe QW with the width $d = 7$ nm [24]. For the validity of our perturbative calculation the following inequality has to be satisfied: $T_*/|M| \ll 1$. In Ref. [24] the ratio $T_*/|M|$ was estimated to be of the order of 10^{-3} for the case mentioned above. Such estimate guarantees validity of the perturbation theory in the exchange interaction.

In the presence of the helical edge states in a 2D TI the IEI between magnetic impurities is determined by the three physically different contributions: contribution due to bulk states [see Eq. (18)], contribution due to edge states [see Eq. (21)], and contribution due to interference between bulk and edge states [see Eqs. (26) and (33)]. With exponential accuracy the spatial dependence of these three contributions can be estimated as

$$H_{\rm IEI}^{\rm bulk} \sim e^{-2R/\xi}, \quad H_{\rm IEI}^{\rm edge} \sim e^{-2|\overline{x}_{AB}|/\xi}, \quad H_{\rm IEI}^{\rm int} \sim e^{-|\overline{x}_{AB}|/\xi - R/\xi_\mu}. \quad (37)$$

We note that for the CdTe/HgTe/CdTe QW with the width $d = 7$ nm the decay length ξ was estimated to be about 40 nm [24]. We mention that ξ is much larger than the decay length for the IEI in a 3D bulk CdTe crystal which is known to be equal to 0.1–1 nm [20]. Contrary to ξ, the other decay length, ξ_μ, depends on the chemical potential μ and ξ_μ can be much larger than ξ for $|M| - |\mu| \ll |M|$.

In the case of two impurities situated deep in the bulk, far away from the edge, the bulk contribution to the IEI dominates. For impurities which are placed near the edge of a 2D TI the main contribution to the IEI is provided by the edge states. However, this edge contribution to the IEI couples only the in-plane components of the impurity spins [16]. At the same time, the interference contribution to the IEI between magnetic impurities situated at the edge involves interaction between z components of the impurity spins [see Eq. (36)]. Although this interaction is exponentially suppressed for the distances along the edge which are larger than ξ_μ and is of the order of $T_*^{(\mu)} = T_*(1-\mu^2/M^2)^{3/2}$, it can become more important than the contribution due to the edge states, Eq. (21), in the case of strong on-site easy axis anisotropy, $H_{\rm anis} = -D_0 S_z^2$ with $D_0 > 0$. The easy axis anisotropy constricts spins to be aligned along the z axis with $\boldsymbol{S}_\parallel = 0$. In Ref. [24] the on-site anisotropy was estimated to be 10^3–10^5 times larger than T_*. Since the IEI between z components of spins is an oscillating function of the distance with the period $2\pi/k_F$ we expect formation of a spin-glass state below the temperature $T_*^{(\mu)}$ for randomly distributed magnetic impurities with the 1D density larger than $1/\xi_\mu$.

Although effects caused by on-site anisotropy might be crucial, the interference contribution to the IEI can be dominant for specific disposition of the impurities even without the anisotropy. Let us consider the following illustrative example: impurity A is located strictly at the edge while the impurity B is displaced at the distance $|x_B| = X$ away from the boundary towards the bulk of a 2D TI. We will suppose that the distance between the impurities along the edge is equal: $y_{AB} = X$. In this situation the three different contributions to the IEI can be estimated as

$$H_{\rm IEI}^{\rm bulk} \sim e^{-2\sqrt{2}X/\xi}, \quad H_{\rm IEI}^{\rm edge} \sim e^{-2X/\xi}, \quad H_{\rm IEI}^{\rm int} \sim e^{-X/\xi} e^{-\sqrt{2}X/\xi_\mu}. \quad (38)$$

Provided $|\mu| > |M|/\sqrt{2}$, the interference contribution to the IEI has the smallest decay length and, therefore, dominates over bulk and edge contributions.

To illustrate the importance of the interference term further, we consider the following situation: the impurity A situated in the bulk at some arbitrary fixed distance x_A from the edge whereas the impurity B can be located anywhere. In this situation for $\mu = 0$ the IEI is always dominated either by the bulk or by the edge contribution. Indeed, this follows from estimates:

$$H_{\rm IEI}^{\rm bulk}/H_{\rm IEI}^{\rm int} \sim H_{\rm IEI}^{\rm int}/H_{\rm IEI}^{\rm edge}.$$

However, for $\mu \neq 0$, the decay length of the interference contribution to the IEI increases in comparison with the case of $\mu = 0$. For some positions of the impurity B, the interference contribution can become the most significant. The comparison

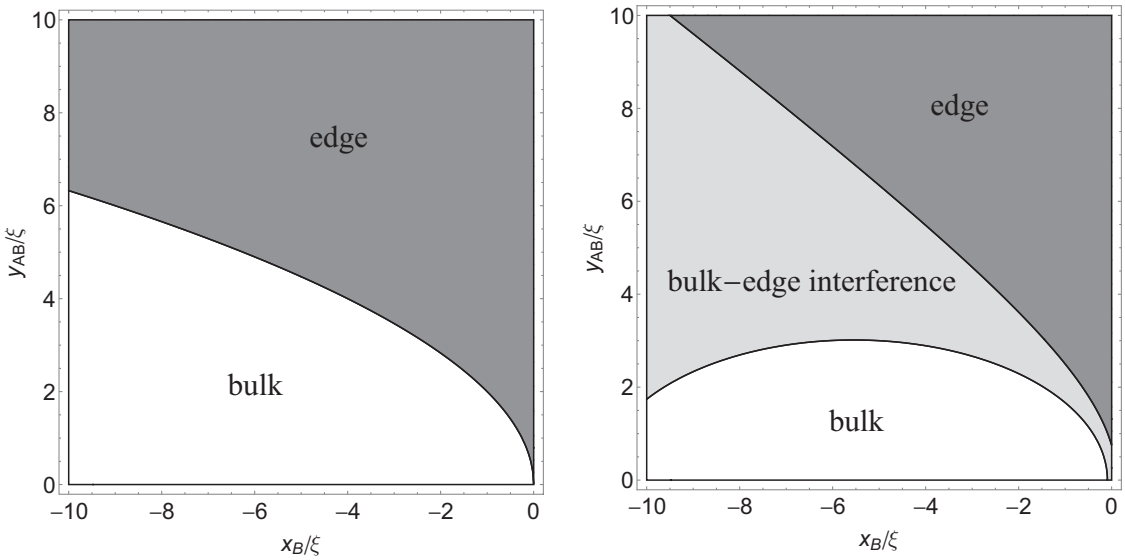

FIG. 3. The regions in which different contributions to the IEI are dominant are presented for the case of $\mu = 0$ (the left figure) and $\mu = 0.6|M|$ (the right figure) for different positions of the impurity B. The impurity A is situated at $|x_A| = \xi$. The white color depicts the dominance of the IEI meditated by the bulk states, the gray color indicates the region in which the interference contribution to the IEI is dominant, and the dark gray color denotes the dominance of the IEI mediated by the edge states.

of the exponential factors for different positions of the impurity B at a given position of the impurity A is shown in Fig. 3. The figure illustrates that for nonzero value of μ there exists the region for which the interference contribution to the IEI is dominant. This area separates the region in which the IEI is mostly due to the bulk states from the region where the interaction due to the edge states is dominant.

Finally, we mention that although the characteristic energy scale T_* of the IEI is rather small, nevertheless, the fine structure of energy levels of a pair of magnetic impurities caused by the IEI can be probed experimentally by broadband electron-spin-resonance technique coupled with an optical detection scheme [39].

To summarize, we studied the IEI between magnetic impurities near the edge of a 2D topological insulator. This interaction can be divided into three physically different contributions. The first contribution is the IEI mediated by the virtual interband transitions of the bulk electron states. It decays exponentially with the distance between the impurities and has two parts: a rotationally invariant part which was analyzed previously in Ref. [24] in detail and the part which is not invariant under in-plane rotations. The latter appears if we take into account the change of the bulk states due to the presence of the edge. The second contribution is the RKKY interaction between the impurities due to the helical edge states of a 2D topological insulator. In accordance with the general expectations this contribution decays with distance between the impurities as a power law and oscillates with the period π/k_F. This contribution is suppressed if both impurities are situated deep in the bulk. This edge contribution couples only in-plane components of the impurity spins. Finally, the last contribution to the IEI can be interpreted as the interaction, mediated by the interference between the bulk and edge states. This term oscillates with k_F and decays exponentially with the distance between the impurities. Interestingly, the decay length of this interference contribution is controlled by the position of the chemical potential within the bulk gap. This fact makes the interference contribution to the IEI dominant in the case of some specific disposition of magnetic impurities.

ACKNOWLEDGMENTS

We thank B. Aronson, M. Durnev, M. Feigel'man, Y. Gefen, M. Glazov, M. Goldstein, G. Min'kov, I. Rozhansky, and, especially, S. Tarasenko, for useful discussions. The work was partially supported by the Russian Foundation for Basic Research under Grant No. 15-52-06005, Russian President Grant No. MD-5620.2016.2, and Russian President Scientific Schools Grant No. NSh-10129.2016.2.

APPENDIX A: THE CONTRIBUTION TO THE IEI DUE TO BULK STATES

In this appendix we present details of the calculation of the contribution due to bulk states to the IEI. Using Eqs. (16), we find the following expression valid at zero temperature:

$$H_{\rm IEI}^{\rm bulk} = \frac{1}{4}\sum_{s,s'=\pm}\int \frac{d\varepsilon}{2\pi}\frac{dk_x}{2\pi}\frac{dk_y}{2\pi}\frac{dz_x}{2\pi}\frac{dz_y}{2\pi}e^{i(k_y-z_y)y_{AB}} \times \frac{\mathrm{Tr}[\mathcal{J}^A\mathcal{B}_s(\boldsymbol{k},x_A,x_B)\mathcal{J}^B\mathcal{B}_{s'}(\boldsymbol{z},x_B,x_A)]}{[i\varepsilon+\mu-s\mathcal{E}(k)][i\varepsilon+\mu-s'\mathcal{E}(z)]}. \quad \text{(A1)}$$

Assuming that the chemical potential is pinned within the bulk gap, we can integrate over energy ε and obtain

$$H_{\rm IEI}^{\rm bulk} = -\frac{1}{4}\sum_{s'=\pm}\int_0^\infty dt\,\mathrm{Tr}[\mathcal{J}^A\tilde{\mathcal{B}}_s(x_A,x_B,y_{AB}) \times \mathcal{J}^B\tilde{\mathcal{B}}_{-s}(x_B,x_A,y_{BA})]. \quad \text{(A2)}$$

Here we introduced integration over an auxiliary variable t and

$$\tilde{\mathcal{B}}_s(x_A,x_B,y_{AB}) = \int \frac{d^2\boldsymbol{k}}{(2\pi)^2}e^{ik_y y_{AB}-t\mathcal{E}(k)}\mathcal{B}_s(\boldsymbol{k},x_A,x_B). \quad \text{(A3)}$$

To proceed further, we need to evaluate the integral over momentum $\boldsymbol{k}$. Since we are interested in the asymptotic behavior of the IEI at large distance, it is enough to evaluate the integral over momentum in the saddle-point approximation. In particular, we shall use the following general result:

$$\int \frac{d^2\boldsymbol{q}}{(2\pi)^2} F(\boldsymbol{q}) e^{i\boldsymbol{q}\boldsymbol{r} - u\sqrt{1+q^2}} \approx \frac{u F(\boldsymbol{q}_0)}{2\pi(r^2+u^2)} e^{-\sqrt{r^2+u^2}}, \quad \text{(A4)}$$

where $\boldsymbol{q}_0 = i\boldsymbol{r}/\sqrt{r^2+u^2}$. This result is valid provided $\sqrt{r^2+u^2} \gg 1$. With the help of Eq. (A4), one finds

$$\tilde{\mathcal{B}}_s(x_A, x_B, y_{AB}) = s \begin{pmatrix} \tilde{I}_{1,s} & \tilde{I}_{2,s} & 0 & 0 \\ -\tilde{I}^*_{2,-s} & -\tilde{I}^*_{1,-s} & 0 & 0 \\ 0 & 0 & \tilde{I}^*_{1,s} & \tilde{I}^*_{2,s} \\ 0 & 0 & -\tilde{I}_{2,-s} & -\tilde{I}_{1,-s} \end{pmatrix}. \quad \text{(A5)}$$

Using the relation $\tilde{\mathcal{B}}_s(x_B, x_A, y_{BA}) = \tilde{\mathcal{B}}^\dagger_s(x_A, x_B, y_{AB})$, one can obtain the expression for $\tilde{\mathcal{B}}_{-s}(x_B, x_A, y_{BA})$ from Eq. (A5) by substituting $-\tilde{I}^*_{1,-s}$ for $\tilde{I}_{1,s}$ and vice versa. Here, the functions $\tilde{I}_1$ and $\tilde{I}_2$ are given as follows:

$$\begin{aligned} \begin{pmatrix} \tilde{I}_{1,s} \\ \tilde{I}_{2,s} \end{pmatrix} &= \begin{pmatrix} -1 + \frac{Ats}{\sqrt{R^2+A^2t^2}} \\ \frac{in_+R}{\sqrt{R^2+A^2t^2}} \end{pmatrix} \frac{e^{-\sqrt{R^2+A^2t^2}/\xi}}{2\pi\xi(R^2+A^2t^2)^{1/2}} \\ &+ \begin{pmatrix} i\left(\frac{\overline{R}\nu_+}{\sqrt{\overline{R}^2+A^2t^2}} + \frac{sAt}{\sqrt{\overline{R}^2+A^2t^2}} - 1\right)^2 \\ \left|\frac{\overline{R}\nu_+}{\sqrt{\overline{R}^2+A^2t^2}} - 1\right|^2 - \frac{2i\nu_y sAt\overline{R}}{\overline{R}^2+A^2t^2} - \frac{A^2t^2}{\overline{R}^2+A^2t^2} \end{pmatrix} \\ &\times \frac{e^{-\sqrt{\overline{R}^2+A^2t^2}/\xi}}{4\pi\xi(\nu_y\overline{R} - isAt)}. \end{aligned} \quad \text{(A6)}$$

We note that under the interchange of the points $\boldsymbol{R}_A$ and $\boldsymbol{R}_B$ the functions $\tilde{I}_{1,s}$ and $\tilde{I}_{2,s}$ transfer to $\tilde{I}^*_{1,s}$ and $-\tilde{I}_{2,s}$, respectively. To perform integration over t, we can simplify expressions for $\tilde{I}_{1,s}$ and $\tilde{I}_{2,s}$ by expanding in t the square root in the exponents and neglecting t in all other places:

$$\begin{aligned} \begin{pmatrix} \tilde{I}_{1,s} \\ \tilde{I}_{2,s} \end{pmatrix} \approx \begin{pmatrix} I_1 \\ I_2 \end{pmatrix} &= \begin{pmatrix} -1 \\ in_+ \end{pmatrix} \frac{1}{2\pi\xi R} e^{-R/\xi - A|M|t^2/2R} \\ &+ \begin{pmatrix} i(\nu_+ - 1)^2 \\ |\nu_+ - 1|^2 \end{pmatrix} \frac{1}{4\pi\xi\nu_y\overline{R}} e^{-\overline{R}/\xi - A|M|t^2/2\overline{R}}. \end{aligned} \quad \text{(A7)}$$

This is allowed provided the following inequalities hold:

$$\frac{R}{\xi} \gg t|M| \gg 1, \qquad \frac{\overline{R}}{\xi} \gg t|M| \gg 1. \quad \text{(A8)}$$

Then using Eqs. (A5) and (A7), we integrate over t (notice that the scale of convergence of the corresponding integrals over t makes inequalities above well justified provided $R/\xi \gg 1$, $\bar{R}/\xi \gg 1$) and obtain

$$H^{\text{bulk}}_{\text{IEI}} = \sum_{a,b=x,y,z} S^A_a K^{\text{bulk}}_{ab} S^B_b, \quad \text{(A9)}$$

where

$$\begin{aligned} K^{\text{bulk}}_{xx} &= J^A_m J^B_m \mathcal{F}_2 - 2J^A_0 J^B_0(\mathcal{F}_2 + \mathcal{F}_3) + \text{c.c.}, \\ K^{\text{bulk}}_{xy} &= -iJ^A_m J^B_m \mathcal{F}_2 - 2iJ^A_0 J^B_0(\mathcal{F}_2 - \mathcal{F}_3) + \text{c.c.}, \\ K^{\text{bulk}}_{xz} &= -2iJ^A_0 J^B_z \mathcal{F}_6 + \text{c.c.}, \\ K^{\text{bulk}}_{yx} &= iJ^A_m J^B_m \mathcal{F}_2 + 2iJ^A_0 J^B_0(\mathcal{F}_2 + \mathcal{F}_3) + \text{c.c.}, \\ K^{\text{bulk}}_{yy} &= J^A_m J^B_m \mathcal{F}_2 - 2J^A_0 J^B_0(\mathcal{F}_2 - \mathcal{F}_3) + \text{c.c.}, \\ K^{\text{bulk}}_{yz} &= 2J^A_0 J^B_z \mathcal{F}_6 + \text{c.c.}, \\ K^{\text{bulk}}_{zx} &= 2iJ^A_z J^B_0 \mathcal{F}_5 + \text{c.c.}, \\ K^{\text{bulk}}_{zy} &= 2J^A_z J^B_0 \mathcal{F}_5 + \text{c.c.}, \\ K^{\text{bulk}}_{zz} &= 2\left[J^A_1\left(\mathcal{F}_1 J^B_1 + \mathcal{F}_4 J^B_2\right) + J^A_2\left(\mathcal{F}_4 J^B_1 + \mathcal{F}_1 J^B_2\right)\right]. \end{aligned} \quad \text{(A10)}$$

Here the functions $\mathcal{F}_{1,\ldots,6}$ are defined as follows:

$$\begin{aligned} \mathcal{F}_1 &= \frac{1}{2}\int_0^\infty dt|I_1|^2 = \mathcal{F}(R,R) + \frac{\overline{R}^2}{4y^2_{AB}}|\nu_+ - 1|^4\mathcal{F}(\overline{R},\overline{R}) \\ &+ i\frac{\overline{R}}{2y_{AB}}\left[(\nu_- - 1)^2 - (\nu_+ - 1)^2\right]\mathcal{F}(R,\overline{R}), \\ \mathcal{F}_2 &= \frac{1}{2}\int_0^\infty dt I_1^2 = \mathcal{F}(R,R) - \frac{\overline{R}^2}{4y^2_{AB}}(\nu_+ - 1)^4\mathcal{F}(\overline{R},\overline{R}) \\ &- i\frac{\overline{R}}{y_{AB}}(\nu_+ - 1)^2\mathcal{F}(R,\overline{R}), \\ \mathcal{F}_3 &= -\frac{1}{2}\int_0^\infty dt I_2^2 = n_+^2\mathcal{F}(R,R) - \frac{\overline{R}^2}{4y^2_{AB}}|\nu_+ - 1|^4\mathcal{F}(\overline{R},\overline{R}) \\ &- i\frac{\overline{R}}{y_{AB}}n_+|\nu_+ - 1|^2\mathcal{F}(R,\overline{R}), \\ \mathcal{F}_4 &= \frac{1}{2}\int_0^\infty dt|I_2|^2 = \mathcal{F}(R,R) + \frac{\overline{R}^2}{4y^2_{AB}}|\nu_+ - 1|^4\mathcal{F}(\overline{R},\overline{R}) \\ &+ i\frac{\overline{R}}{2y_{AB}}(n_+ - n_-)|\nu_+ - 1|^2\mathcal{F}(R,\overline{R}), \\ \mathcal{F}_5 &= \frac{1}{2}\int_0^\infty dt I_1^* I_2 = -in_+\mathcal{F}(R,R) \\ &- i\frac{\overline{R}^2}{4y^2_{AB}}(\nu_- - 1)^2|\nu_+ - 1|^2\mathcal{F}(\overline{R},\overline{R}) \\ &+ \frac{\overline{R}}{2y_{AB}}\left[n_+(\nu_- - 1)^2 - |\nu_+ - 1|^2\right]\mathcal{F}(R,\overline{R}), \\ \mathcal{F}_6 &= -\frac{1}{2}\int_0^\infty dt I_1^* I_2^* = -in_-\mathcal{F}(R,R) \\ &+ i\frac{\overline{R}^2}{4y^2_{AB}}(\nu_- - 1)^2|\nu_+ - 1|^2\mathcal{F}(\overline{R},\overline{R}) \\ &+ \frac{\overline{R}}{2y_{AB}}\left[n_-(\nu_- - 1)^2 + |\nu_+ - 1|^2\right]\mathcal{F}(R,\overline{R}). \end{aligned} \quad \text{(A11)}$$

The function $\mathcal{F}(R,R')$ describes the exponential decay of the IEI:

$$\mathcal{F}(R,R') = \frac{|M|^3}{16A^4}\sqrt{\frac{2\xi^3}{\pi^3 RR'(R+R')}}\, e^{-R/\xi - R'/\xi}. \quad \text{(A12)}$$

The result (A10) is valid provided the following inequalities are fulfilled:

$$R \gg \xi, \qquad \overline{R} \gg \xi. \tag{A13}$$

In the case of both impurities located in the bulk far away from the boundary, $|x_A|, |x_B| \gg \xi$, i.e., the distance $R \ll \overline{R}$, the result (A10) transforms into the expression (18).

APPENDIX B: INTERFERENCE CONTRIBUTION TO THE IEI

In this appendix we present details of derivation of the interference contribution to the IEI. Using Eqs. (10) and (14), we can express the interference contribution to the IEI at zero temperature and for $y_{AB} > 0$ as follows:

$$H_{\mathrm{IEI}}^{\mathrm{int}} = \frac{i|M|}{2A^2} e^{-|\overline{x}_{AB}|/\xi} \sum_{s,s'=\pm} \int \frac{d\varepsilon}{2\pi} \int \frac{d^2\boldsymbol{k}}{(2\pi)^2} \frac{s'\theta(-s'\varepsilon)}{i\varepsilon + \mu - s\mathcal{E}(k)} e^{s'(\varepsilon - i\mu)y_{AB}/A} [e^{ik_y y_{AB}} \operatorname{Tr} \mathcal{J}^A \mathcal{B}_s(\boldsymbol{k}, x_A, x_B) \mathcal{J}^B \Gamma_{-s'}$$
$$+ e^{ik_y y_{BA}} \operatorname{Tr} \mathcal{J}^A \Gamma_{s'} \mathcal{J}^B \mathcal{B}_s(\boldsymbol{k}, x_B, x_A)]. \tag{B1}$$

After introducing an integration over a variable t to raise the denominator $i\varepsilon + \mu - s\mathcal{E}(k)$ into the exponent, we can integrate over ε and obtain

$$H_{\mathrm{IEI}}^{\mathrm{int}} = -\frac{|M|}{4\pi A^2} e^{-|\overline{x}_{AB}|/\xi} \sum_{s,s'=\pm} \int_0^\infty dt \, \frac{e^{is'k_F y_{AB} + s\mu t}}{t + iss' y_{AB}/A} \operatorname{Tr}\left[\mathcal{J}^A \tilde{\mathcal{B}}_s(x_A, x_B, y_{AB}) \mathcal{J}^B \Gamma_{s'} + \mathcal{J}^A \Gamma_{-s'} \mathcal{J}^B \tilde{\mathcal{B}}_s(x_B, x_A, y_{BA})\right]. \tag{B2}$$

Next, we find

$$H_{\mathrm{IEI}}^{\mathrm{int}} = \textstyle\sum_{s'=\pm} \operatorname{Tr}\left[\mathcal{J}^A \hat{\mathcal{B}}_{s'}(x_A, x_B, y_{AB}) \mathcal{J}^B \Gamma_{s'} + \mathcal{J}^B \hat{\mathcal{B}}_{s'}^\dagger(x_A, x_B, y_{AB}) \mathcal{J}^A \Gamma_{s'}\right], \tag{B3}$$

where

$$\hat{\mathcal{B}}_{s'}(x_A, x_B, y_{AB}) = -\frac{|M|}{4\pi A^2} e^{-|\overline{x}_{AB}|/\xi} \sum_{s=\pm} \int_0^\infty dt \, \frac{e^{is'k_F y_{AB} + s\mu t}}{t + iss' y_{AB}/A} \tilde{\mathcal{B}}_s(x_A, x_B, y_{AB}). \tag{B4}$$

After inspection of Eq. (A6), we see that one can evaluate the integral over t within the saddle-point approximation, provided R and $\overline{R}$ are large enough. We note that in the sum over s the term with $s = \operatorname{sgn} \mu$ yields the leading contribution only. In particular, we use the following result for $1 > a > 0$:

$$\int_0^\infty du \, F(u) e^{au - \sqrt{r^2 + u^2}} \approx \frac{\sqrt{2\pi r}}{(1-a^2)^{3/4}} F(u_0) e^{-r\sqrt{1-a^2}}, \tag{B5}$$

where $u_0 = ar/\sqrt{1-a^2}$. This saddle-point result is valid provided $r \gg 1/(a^2\sqrt{1-a^2})$. In terms of R and $\overline{R}$ this condition implies that $R, \overline{R} \gg \xi(M^3/\mu^2\sqrt{M^2 - \mu^2})$.

Performing integration over t in Eq. (B4) with the help of the saddle-point result (B5), we find

$$\hat{\mathcal{B}}_{s'}(x_A, x_B, y_{AB}) = \frac{e^{is'k_F y_{AB}}}{\sin\theta_\mu + is'n_y \cos\theta_\mu} F_\mu(\boldsymbol{R}) \begin{pmatrix} 1 - \sin\theta_\mu & -in_+ \cos\theta_\mu & 0 & 0 \\ -in_- \cos\theta_\mu & -1 - \sin\theta_\mu & 0 & 0 \\ 0 & 0 & 1 - \sin\theta_\mu & in_- \cos\theta_\mu \\ 0 & 0 & in_+ \cos\theta_\mu & -1 - \sin\theta_\mu \end{pmatrix}$$
$$- \frac{e^{is'k_F y_{AB}} F_\mu(\overline{\boldsymbol{R}})}{\sin\theta_\mu + is'v_y \cos\theta_\mu} \begin{pmatrix} u_\mu & v_\mu & 0 & 0 \\ -v_{-\mu}^* & -u_{-\mu}^* & 0 & 0 \\ 0 & 0 & u_\mu^* & v_\mu^* \\ 0 & 0 & -v_{-\mu} & -u_{-\mu} \end{pmatrix}. \tag{B6}$$

Next, performing summation over s', we obtain the results (26) and (33): the first term in Eq. (B6) results in the invariant part of the interference IEI (26), while the second term results in the noninvariant part (33) [see Eq. (24)].

APPENDIX C: INTERFERENCE CONTRIBUTION TO THE IEI BETWEEN THE IMPURITIES SITUATED EXACTLY AT THE EDGE

In this Appendix we present details of derivation of the interference contribution to the IEI for magnetic impurities situated exactly at the edge of the 2D topological insulator, i.e., for the case $x_A = x_B = 0$. In this case the expressions (A6) for the

integrals $\tilde{I}_{1,s}$ and $\tilde{I}_{2,s}$ vanish identically. Therefore, one has to compute the integrals over $\boldsymbol{k}$ more accurately. We find that

$$\tilde{I}_{1,s} = i\tilde{I}_{2,s} = \int \frac{d^2\boldsymbol{k}}{(2\pi)^2} e^{isk_y y_{AB} - t\mathcal{E}(k)} \frac{sA^2k_x^2}{\mathcal{E}(k)[\mathcal{E}(k) + Ak_y]}. \tag{C1}$$

Evaluating the integral over $\boldsymbol{k}$ in the saddle-point approximation, we find

$$\tilde{I}_{1,s} = i\tilde{I}_{2,s} = \frac{s}{2\pi} \frac{1}{At + isy_{AB}} \frac{e^{-\sqrt{y_{AB}^2 + A^2t^2}}}{\sqrt{y_{AB}^2 + A^2t^2}}. \tag{C2}$$

Performing integration over t in Eq. (B4) with the help of Eq. (B5), we find

$$\hat{\mathcal{B}}_{s'}(0,0,y_{AB}) = s' e^{is'k_F y_{AB} + is'\theta_\mu} \frac{\xi \cos\theta_\mu}{y_{AB}} F_\mu(0,y_{AB}) \begin{pmatrix} e^{i\theta_\mu} & -ie^{i\theta_\mu} & 0 & 0 \\ ie^{i\theta_\mu} & e^{i\theta_\mu} & 0 & 0 \\ 0 & 0 & -e^{-i\theta_\mu} & -ie^{-i\theta_\mu} \\ 0 & 0 & ie^{-i\theta_\mu} & -e^{-i\theta_\mu} \end{pmatrix}. \tag{C3}$$

Using this expression, we find the result (36) for the interference contribution to the IEI for the case of magnetic impurities situated exactly at the edge.

[1] X.-L. Qi and S.-C. Zhang, Topological insulators and superconductors, Rev. Mod. Phys. **83**, 1057 (2011).

[2] M. Z. Hasan and C. L. Kane, *Colloquium*: Topological insulators, Rev. Mod. Phys. **82**, 3045 (2010).

[3] C. L. Kane and E. J. Mele, Z_2 Topological Order and the Quantum Spin Hall Effect, Phys. Rev. Lett. **95**, 146802 (2005).

[4] B. A. Bernevig, T. L. Hughes, and S.-C. Zhang, Quantum spin Hall effect and topological phase transition in HgTe quantum wells, Science **314**, 1757 (2006).

[5] M. König, S. Wiedmann, C. Brüne, A. Roth, H. Buhmann, L. W. Molenkamp, X.-L. Qi, and S.-C. Zhang, Quantum spin Hall insulator state in HgTe quantum wells, Science **318**, 766 (2007).

[6] J. I. Väyrynen, M. Goldstein, and L. I. Glazman, Helical Edge Resistance Introduced by Charge Puddles, Phys. Rev. Lett. **110**, 216402 (2013).

[7] J. I. Väyrynen, M. Goldstein, Y. Gefen, and L. I. Glazman, Resistance of helical edges formed in a semiconductor heterostructure, Phys. Rev. B **90**, 115309 (2014).

[8] N. Kainaris, I. V. Gornyi, S. T. Carr, and A. D. Mirlin, Conductivity of a generic helical liquid, Phys. Rev. B **90**, 075118 (2014).

[9] J. Wang, Y. Meir, and Y. Gefen, Spontaneous breakdown of topological protection in two dimensions, Phys. Rev. Lett. **118**, 046801 (2017).

[10] J. Maciejko, Ch. Liu, Y. Oreg, X.-L. Qi, C. Wu, and S.-C. Zhang, Kondo Effect in the Helical Edge Liquid of the Quantum Spin Hall State, Phys. Rev. Lett. **102**, 256803 (2009).

[11] Y. Tanaka, A. Furusaki, and K. A. Matveev, Conductance of a Helical Edge Liquid Coupled to a Magnetic Impurity, Phys. Rev. Lett. **106**, 236402 (2011).

[12] J. Maciejko, Kondo lattice on the edge of a two-dimensional topological insulator, Phys. Rev. B **85**, 245108 (2012).

[13] V. Cheianov and L. I. Glazman, Mesoscopic Fluctuations of Conductance of a Helical Edge Contaminated by Magnetic Impurities, Phys. Rev. Lett. **110**, 206803 (2013).

[14] B. L. Altshuler, I. L. Aleiner, and V. I. Yudson, Localization at the Edge of a 2d Topological Insulator by Kondo Impurities with Random Anisotropies, Phys. Rev. Lett. **111**, 086401 (2013).

[15] O. M. Yevtushenko, A. Wugalter, V. I. Yudson, and B. L. Altshuler, Transport in helical luttinger liquid with Kondo impurities, Europhys. Lett. **112**, 57003 (2015).

[16] Y.-W. Lee and Y.-L. Lee, Electrical control and interaction effects of the RKKY interaction in helical liquids, Phys. Rev. B **91**, 214431 (2015).

[17] M. A. Ruderman and C. Kittel, Indirect exchange coupling of nuclear magnetic moments by conduction electrons, Phys. Rev. **96**, 99 (1954).

[18] T. Kasuya, A theory of metallic ferro- and antiferromagnetism on Zener's model, Prog. Theor. Phys. **16**, 45 (1956).

[19] K. Yosida, Magnetic properties of Cu-Mn alloys, Phys. Rev. **106**, 893 (1957).

[20] N. Bloembergen and T. J. Rowland, Nuclear spin exchange in solids: Tl^{203} and Tl^{205} magnetic resonance in thallium and thallic oxide, Phys. Rev. **97**, 1679 (1955).

[21] I. Ya. Korenblit and E. F. Shender, Ferromagnetism of disordered systems, Sov. Phys. Usp. **21**, 832 (1978).

[22] A. A. Abrikosov, Spin glasses with short range interaction, Adv. Phys. **29**, 869 (1980).

[23] T. Kernreiter, M. Governale, U. Zülicke, and E. M. Hankiewicz, Anomalous Spin Response and Virtual-Carrier-Mediated Magnetism in a Topological Insulator, Phys. Rev. X **6**, 021010 (2016).

[24] P. D. Kurilovich, V. D. Kurilovich, and I. S. Burmistrov, Indirect exchange interaction between magnetic impurities in the two-dimensional topological insulator based on CdTe/HgTe/CdTe quantum wells, Phys. Rev. B **94**, 155408 (2016).

[25] Q. Liu, C.-X. Liu, C. Xu, X.-L. Qi, and S.-C. Zhang, Magnetic Impurities on the Surface of a Topological Insulator, Phys. Rev. Lett. **102**, 156603 (2009).

[26] F. Ye, G. H. Ding, H. Zhai, and Z. B. Su, Spin helix of magnetic impurities in two-dimensional helical metal, Europhys. Lett. **90**, 47001 (2010).

[27] I. Garate and M. Franz, Magnetoelectric response of the time-reversal invariant helical metal, Phys. Rev. B **81**, 172408 (2010).

[28] R. R. Biswas and A. V. Balatsky, Impurity-induced states on the surface of three-dimensional topological insulators, Phys. Rev. B **81**, 233405 (2010).

[29] D. A. Abanin and D. A. Pesin, Ordering of Magnetic Impurities and Tunable Electronic Properties of Topological Insulators, Phys. Rev. Lett. **106**, 136802 (2011).

[30] J.-J. Zhu, D.-X. Yao, S.-C. Zhang, and K. Chang, Electrically Controllable Surface Magnetism on the Surface of Topological Insulators, Phys. Rev. Lett. **106**, 097201 (2011).

[31] D. K. Efimkin and V. Galitski, Self-consistent theory of ferromagnetism on the surface of a topological insulator, Phys. Rev. B **89**, 115431 (2014).

[32] V. I. Litvinov, Oscillating Bloembergen-Rowland interaction in three-dimensional topological insulators, Phys. Rev. B **94**, 035138 (2016).

[33] X. Dai, T. L. Hughes, X.-L. Qi, Z. Fang, and S.-C. Zhang, Helical edge and surface states in HgTe quantum wells and bulk insulators, Phys. Rev. B **77**, 125319 (2008).

[34] R. Winkler, L. Y. Wang, Y. H. Lin, and C. S. Chu, Robust level coincidences in the subband structure of quasi-2D systems, Solid State Commun. **152**, 2096 (2012).

[35] L. Weithofer and P. Recher, Chiral Majorana edge states in HgTe quantum wells, New J. Phys. **15**, 085008 (2013).

[36] S. A. Tarasenko, M. V. Durnev, M. O. Nestoklon, E. L. Ivchenko, J.-W. Luo, and A. Zunger, Split Dirac cones in HgTe/CdTe quantum wells due to symmetry-enforced level anticrossing at interfaces, Phys. Rev. B **91**, 081302 (2015).

[37] D. G. Rothe, R. W. Reinthaler, C.-X. Liu, L. W. Molenkamp, S.-C. Zhang, and E. M. Hankiewicz, Fingerprint of different spin-orbit terms for spin transport in HgTe quantum wells, New J. Phys. **12**, 065012 (2010).

[38] B. A. Volkov and O. A. Pankratov, Two-dimensional massless electrons in an inverted contact, JETP Lett. **42**, 178 (1985).

[39] C. Laplane, E. Zambrini Cruzeiro, F. Fröwis, P. Goldner, and M. Afzelius, High-Precision Measurement of the Dzyaloshinsky-Moriya Interaction Between Two Rare-Earth ions in a Solid, Phys. Rev. Lett. **117**, 037203 (2016).